Journal of Power Sources 244 (2013) 266–271

Contents lists available at SciVerse ScienceDirect

Journal of Power Sources

journal homepage: www.elsevier.com/locate/jpowsour

Effect of ionic liquid as a flame-retarding additive on the cycling performance and thermal stability of lithium-ion batteries

Seo-Youn Bae [a], Eun-Gi Shim [b], Dong-Won Kim [a,*]

[a] Department of Chemical Engineering, Hanyang University, Seungdong-Gu, Seoul 133-791, Republic of Korea
[b] Electrolyte Development Team, Soulbrain Co. Ltd, Yongin-si, Gyeonggi-do 446-599, Republic of Korea

HIGHLIGHTS

- ► Different ionic liquids are added as a flame-retarding additive to base electrolyte.
- ► Addition of ionic liquid reduces the flammability and improves the thermal stability.
- ► BMP–PF_6 is the best flame-retarding ionic liquid for good cycling performance.

ARTICLE INFO

Article history:
Received 2 October 2012
Received in revised form
2 January 2013
Accepted 14 January 2013
Available online 31 January 2013

Keywords:
1-Butyl-1-methylpyrrolidinium
Ionic liquid
Flame-retarding additive
Lithium-ion cell
Thermal stability

ABSTRACT

Different ionic liquids based on the 1-butyl-1-methylpyrrolidinium cation are added as a flame-retarding additive to a standard organic electrolyte, and their influences on the cycling performance and thermal stability of lithium-ion cells are investigated. The self-extinguishing time and DSC results demonstrate that the addition of the ionic liquids to the base electrolyte is effective in reducing the flammability of the electrolyte solution and improving the thermal stability of the cell. Among the ionic liquids evaluated in this study, 1-butyl-1-methylpyrrolidinium hexafluorophosphate was the most desirable flame-retarding additive for achieving the best cycling performance of lithium-ion cell.

© 2013 Elsevier B.V. All rights reserved.

1. Introduction

Lithium-ion batteries have rapidly become the most common power source for portable electronic devices, power tools and electric vehicles due to their high energy density and good cycling stability. However, safety is one of the crucial issues that must be addressed before they can be widely used to fabricate large cells for use in electric vehicles and energy storage systems. Unfortunately, the high flammability of organic solvents used in common liquid electrolytes may be the major possible cause of fires and explosions when short circuits or local overheating accidently occurs. In order to improve the safety of the cells, recent investigations have focused on the development of less-flammable electrolytes containing flame-retarding additives such as phosphates, phosphazenes, borates, siloxanes, fluorinated carbonates, fluorinated ethers and ionic liquids [1–10]. As a flame-retarding additive, ionic liquids have attractive properties including negligible vapor pressure, low flammability and high thermal stability. Ionic liquids are generally composed of organic ions that may undergo almost unlimited structural variations where the selection of the cation and anion has a drastic effect on their physicochemical properties [11–13]. For lithium battery applications, great attention has been paid to ionic liquids based on pyrrolidinium cations due to their reasonably wide electrochemical stability and high ionic conductivity [14–18]. Despite the many studies conducted on these ionic liquids, there are no rigorous reports available concerning the effect of the anion in the ionic liquids on the electrochemical performance of lithium-ion cells.

With the goal of developing less-flammable electrolytes to result in safe lithium-ion batteries, different ionic liquids were added as a flame-retarding additive into the base electrolyte. In this study, we selected 1-butyl-1-methylpyrrolidinium (BMP) as the cation and bis(trifluoromethylsulfonyl) imide (TFSI), hexafluorophosphate (PF_6), and tetrafluoroborate (BF_4) as anions. Using these less-

---

* Corresponding author. Tel.: +82 2 2220 2337; fax: +82 2 2298 4101.
E-mail address: dongwonkim@hanyang.ac.kr (D.-W. Kim).

0378-7753/$ – see front matter © 2013 Elsevier B.V. All rights reserved.
http://dx.doi.org/10.1016/j.jpowsour.2013.01.100

flammable electrolytes, we assembled lithium-ion cells composed of a carbon anode and a $LiCoO_2$ cathode. The cycling performances of the cells were evaluated and compared to that of the cell assembled with the base liquid electrolyte. The influences of the different anions on the cycling characteristics and thermal stability of the cells were investigated.

2. Experimental

2.1. Electrolyte preparation

BMP–TFSI, BMP–PF_6 and BMP–BF_4 were purchased from Chem Tech Research Incorporation, Korea and were used after drying under vacuum at 50 °C for 24 h. The base electrolyte, 1.15 M $LiPF_6$ in ethylene carbonate (EC)/diethyl carbonate (DEC) (3:7 by volume, battery grade) containing 1 wt.% vinylene carbonate (VC), was kindly supplied by Soulbrain Co. Ltd., Korea and used without further treatment. Each ionic liquid was directly added to the base electrolyte at a concentration of 10 wt.% in an Ar-filled glove box. In order to improve the wettability of the polyethylene separator for the electrolyte solution, a porous poly(vinylidene fluoride-*co*-hexafluoropropylene)-coated polyethylene separator was prepared according to a procedure reported previously [19]. The polymer-coated separator was easily wetted by the electrolyte solution and retained the electrolyte solution well.

2.2. Electrode preparation and cell assembly

The cathode was prepared by coating an *N*-methyl pyrrolidone (NMP)-based slurry containing $LiCoO_2$ (Japan Chemical), PVdF and super-P carbon (85:7.5:7.5) onto aluminum foil. Its active mass loading corresponded to a capacity of about 1.0 mAh cm^{-2}. The carbon anode was prepared by coating an NMP-based slurry of mesocarbon microbeads (MCMB, Osaka gas), PVdF, and super-P carbon (88:8:4) onto copper foil. The coin-type cell (CR2032) composed of a carbon anode, a polymer-coated separator, and a $LiCoO_2$ cathode was assembled in the electrolyte solution. All cells were assembled in a dry box filled with argon gas. After the cell assembly, the cells were kept at 25 °C for 12 h to imbue the electrodes with the electrolyte solution.

2.3. Measurements

The conductivity measurements of the electrolyte solutions were performed using a Cond 3210 conductivity meter (WTW GmbH, Germany). The self-extinguishing time (SET) was measured to quantify the flammability of the electrolyte solution, as previously described [20]. Briefly, the SET value was obtained by igniting the pre-weighed electrolytes soaked in an inert glass-fiber wick, followed by measuring the time required for the flame to be extinguished. The electrolyte was judged to be non-flammable if the electrolyte did not ignite during the testing or if the ignition of the electrolyte ceased when the flame source was removed [4,21,22]. Linear sweep voltammetry (LSV) was performed to investigate the electrochemical stability of the electrolyte solution on a stainless working electrode, with counter and reference electrodes of lithium metal, at a scanning rate of 1.0 m V s^{-1}. Charge and discharge cycling tests of the lithium-ion cells were conducted over a voltage range of 3.0–4.2 V with battery test equipment (WBCS 3000, Wonatech, Korea). For the differential scanning calorimetry (DSC) measurements of the delithiated $Li_{1-x}CoO_2$ materials, the cells were fully recharged to 4.2 V after 100 cycles and were disassembled in a dry room. The cathode materials scraped from the current collector were rinsed with dimethyl carbonate (DMC) to remove the residual electrolyte and dried under vacuum. The resulting electrodes were sealed together with the electrolyte solution in a hermetic stainless steel pan, and measurements were performed at a heating rate of 5 °C min^{-1}. The amount of electrolyte solution was 30 wt.% based on the cathode material and the heat flow was calculated based on the weight of the cathode active material. The surface morphology of the $LiCoO_2$ cathodes after 100 cycles was examined using a field emission scanning electron microscope (FE-SEM, JEOL, JSM-6330F) and transmission electron microscopy (TEM, JEOL, JEM-2100).

3. Results and discussion

Fig. 1 shows the ionic conductivities of the base electrolyte and electrolyte solutions containing the different ionic liquids. The ionic conductivity of the base electrolyte was 6.8×10^{-3} S cm^{-1}. When 10 wt.% ionic liquid (BMP–TFSI, BMP–BF_4) was added to the base electrolyte, the ionic conductivities were slightly decreased since the addition of the ionic liquid increased the viscosity of the resulting electrolyte solution due to the increased ion–solvent and coulombic interactions between the ionic species. On the other hand, the electrolyte solution containing 10 wt.% BMP–PF_6 showed a higher ionic conductivity than the base electrolyte, which may be because of the increase in the number of free ions arising from the dissociation of BMP–PF_6 surpassing the decrease of the ionic mobility in the electrolyte solution. In order to compare the flammable behavior of the electrolyte solution containing the different ionic liquids, flammability tests were performed. As shown previously [20,23], the flammability of a given electrolyte solution is proportional to the SET value. The SET values of the different electrolyte solutions are shown in Fig. 1. The ionic liquids considered in this study did not exhibit any combustion, even during ignition with a flame source (i.e., their SET values are 0 s g^{-1}), indicating all of them are non-flammable. When the ionic liquid was added into the base electrolyte, both the burning time and the flame intensity decreased, resulting in reduced flammability. Accordingly, the SET values of the electrolyte solution decreased by adding the ionic liquids. These results suggest that addition of the non-flammable ionic liquids to base electrolyte is effective in reducing the flammability of the electrolyte.

Linear sweep voltammetry curves of the different electrolyte solutions obtained from the cathodic and anodic scans are shown in Fig. 2(a) and (b), respectively. It can be seen in Fig. 2(a) that the cathodic current starts to increase slightly at around 1.6 V *vs.* Li/Li^+ in the case of the base electrolyte without an ionic liquid. This behavior can be attributed to the reductive decomposition of VC, which results in the formation of a stable solid electrolyte interphase (SEI) layer [18]. In the electrolyte solution containing an ionic

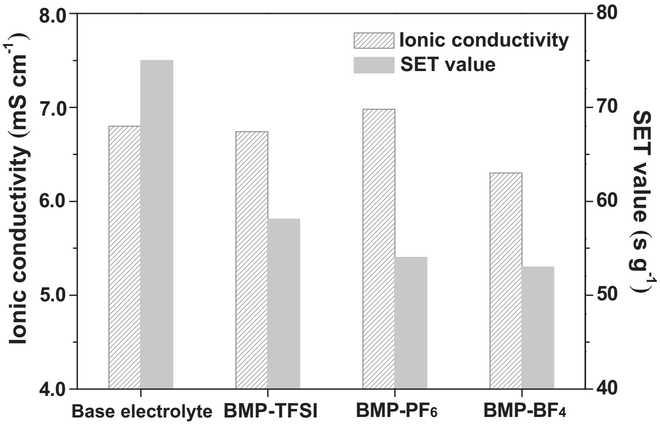

Fig. 1. Ionic conductivities and SET values of the electrolyte solutions containing different ionic liquids.

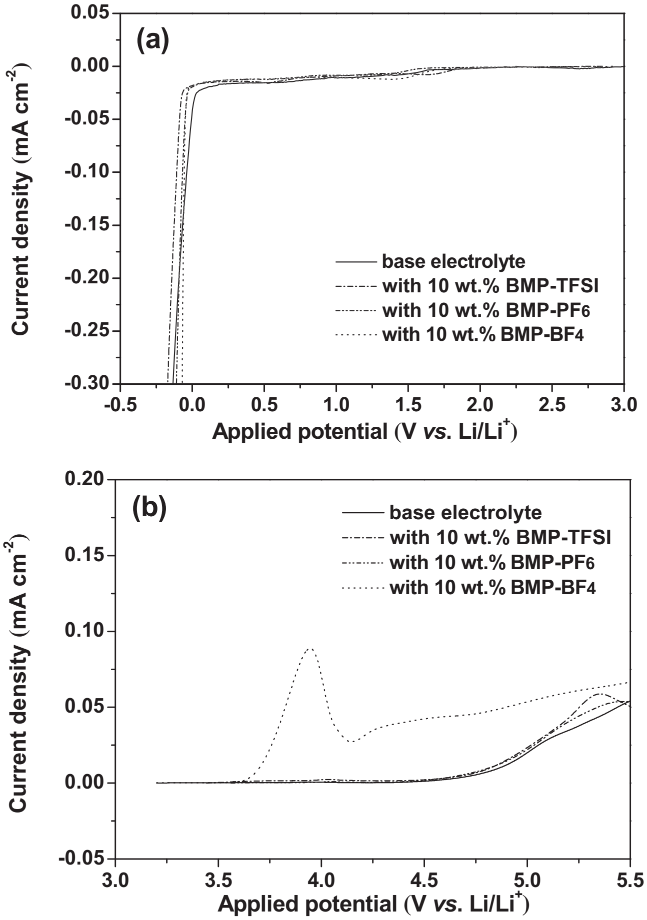

Fig. 2. Linear sweep voltammograms of the different electrolyte solutions: (a) cathodic scan and (b) anodic scan.

liquid, there are no significant reductive peaks corresponding to the reductive decomposition of the ionic liquid. This indicates that VC electrochemically decomposes to form an effective SEI before the decomposition of the ionic liquid (BMP–TFSI, BMP–PF_6, BMP–BF_4) occurs in the electrolyte solution and kinetically extends the cathodic stability of the electrolyte to 0 V *vs.* Li/Li^+. This result is consistent with previous works which showed that carbonate-based solvents could effectively prevent decomposition of ionic liquids [18,24–27]. In the anodic scan shown in Fig. 2(b), the oxidative current corresponding to the anodic decomposition of the electrolyte starts at around 4.7 V for the base electrolyte without ionic liquid. The addition of BMP–TFSI or BMP–PF_6 into the base electrolyte hardly affected the anodic stability of the electrolyte solution. On the other hand, a relatively large and broad oxidation peak was observed in the potential range between 3.6 and 4.1 V for the electrolyte solution containing BMP–BF_4, which may originate from the oxidative decomposition of BMP–BF_4.

The cycling performances of lithium-ion cells assembled with electrolyte solutions containing the different ionic liquids were evaluated. The assembled cells were initially subjected to a preconditioning cycle with a cut-off voltage of 3.0–4.2 V at a 0.1 C rate and their cycling curves are shown in Fig. 3. The first discharge capacity of the lithium-ion cell using the base electrolyte was 146.2 mAh g^{-1} based on the $LiCoO_2$ active cathode material. The discharge capacities of the lithium-ion cells assembled with electrolyte solutions containing the ionic liquids ranged from 123.1 to 145.9 mAh g^{-1}, depending on the type of ionic liquid. It should be noted that both the discharge capacity and the cycling efficiency were the lowest in the cell with the electrolyte containing BMP–BF_4. In this cell, an irreversible charge plateau could be clearly observed at around 2.0 V, which may arise from the irreversible oxidative decomposition of BMP–BF_4 at the $LiCoO_2$ cathode because the cathode may be attained at the oxidative decomposition potential of BMP–BF_4 ($\sim$3.6 V) shown in Fig. 2(b).

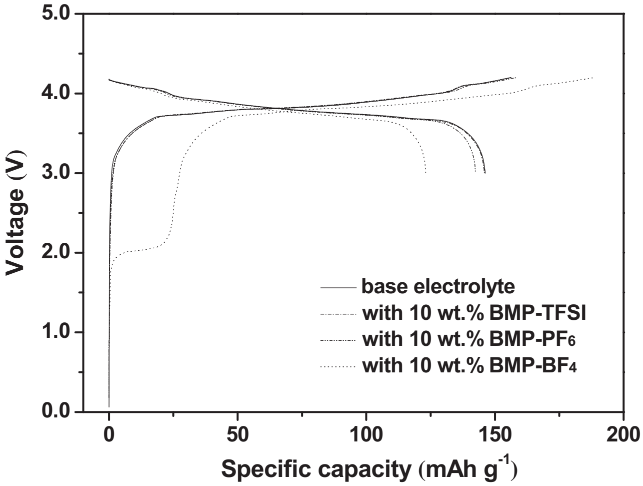

Fig. 3. First preconditioning charge–discharge curves of lithium-ion cells assembled with different electrolyte solutions (current rate: 0.1 C, cut-off: 3.0–4.2 V).

After two preconditioning cycles, the cell was charged at a constant current rate of 0.5 C to 4.2 V. This was followed by a constant voltage charge with decreasing current until a final current equal to 20% of the charging current was reached. The cell was then discharged to 3.0 V at the same current rate (0.5 C). Fig. 4 shows the charge–discharge curves of the 1st, 10th, 20th, 50th, and 100th cycles of the lithium-ion cell assembled with the electrolyte solution containing 10 wt.% BMP–PF_6. The cell had a first discharge capacity of 141.5 mAh g^{-1} and the cycling efficiency steadily increased with increasing cycle number. Fig. 5 shows the discharge capacity as a function of the cycle number in the cells prepared with electrolyte solutions containing the different ionic liquids. It can be seen that the cycling characteristics of the cells are dependent on the type of ionic liquid in the electrolyte solution. With respect to the discharge capacity and capacity retention, the cycling behavior

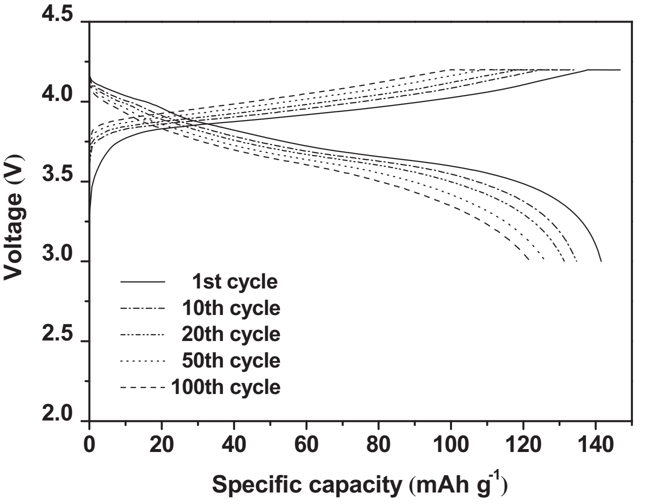

Fig. 4. Charge and discharge curves of the lithium-ion cell assembled with the electrolyte solution containing 10 wt.% BMP–PF_6 (0.5 C CC and CV charge, 0.5 C CC discharge, cut-off: 3.0–4.2 V).

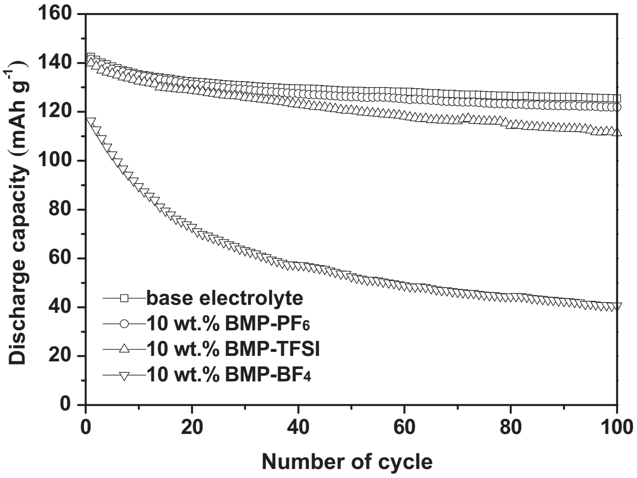

Fig. 5. Discharge capacities as a function of the cycle number for lithium-ion cells assembled with the different electrolyte solutions (room temperature, 0.5 C CC and CV charge, 0.5 C CC discharge, cut-off voltage range: 3.0–4.2 V).

of the cell containing BMP–PF_6 or BMP–TFSI was comparable to that of the cell assembled with the base liquid electrolyte. Good cycling performance of the cells with electrolyte containing BMP–PF_6 or BMP–TFSI is attributed to the high ionic conductivity and good electrochemical stability of the electrolyte solution, as illustrated in Figs. 1 and 2. On the other hand, the cell with BMP–BF_4 showed a low initial discharge capacity and significant capacity fading during cycling. As explained earlier, the addition of BMP–BF_4 may cause undesirable and irreversible decomposition reactions of ionic liquid on the electrode surface during cycling, resulting in a low initial capacity and a large capacity decline. In consideration of the initial discharge capacity and capacity retention, BMP–PF_6 is the most desirable ionic liquid as a flame-retarding additive.

To clarify the influence of the ionic liquids on the morphologies of the $LiCoO_2$ cathode after repeated cycling, SEM analysis was carried out and the results are shown in Fig. 6. There are no significant differences between the SEM images of the cathodes with the base electrolyte and electrolyte solutions containing BMP–TFSI or BMP–PF_6. On the contrary, the cathode cycled in the electrolyte solution containing BMP–BF_4 seems to be covered with a relatively thick surface layer, which may be formed by the oxidative decomposition of BMP–BF_4 on the electrode surface. In order to provide a higher magnification image showing the presence of the surface film on the cathode active materials, the TEM images of the $LiCoO_2$ particles were investigated and compared. Fig. 7 shows the TEM images of the $LiCoO_2$ active materials obtained after 100 cycles of the cells assembled with different electrolytes. A magnified image around the edge of the $LiCoO_2$ particle clearly reveals that it is uniformly covered with surface layer. The addition of BMP–TFSI or BMP–PF_6 into the base electrolyte seems to hardly affect a thickness of the surface layer formed on $LiCoO_2$ material. On the other hand, a relatively thick surface layer ($\sim$35 nm) is observed on $LiCoO_2$ material cycled in the electrolyte solution containing BMP–BF_4, which may originate from the oxidative decomposition of BMP–BF_4 during repeated cycling. These results provide conclusive evidence that the $LiCoO_2$ particle is covered with thick surface layer formed by irreversible oxidation of BMP–BF_4. Accordingly, in the presence of BMP–BF_4, the resistive surface film on the cathode hampers charge transport at the electrode and electrolyte interface, which causes a capacity decline with cycling, as shown in Fig. 5.

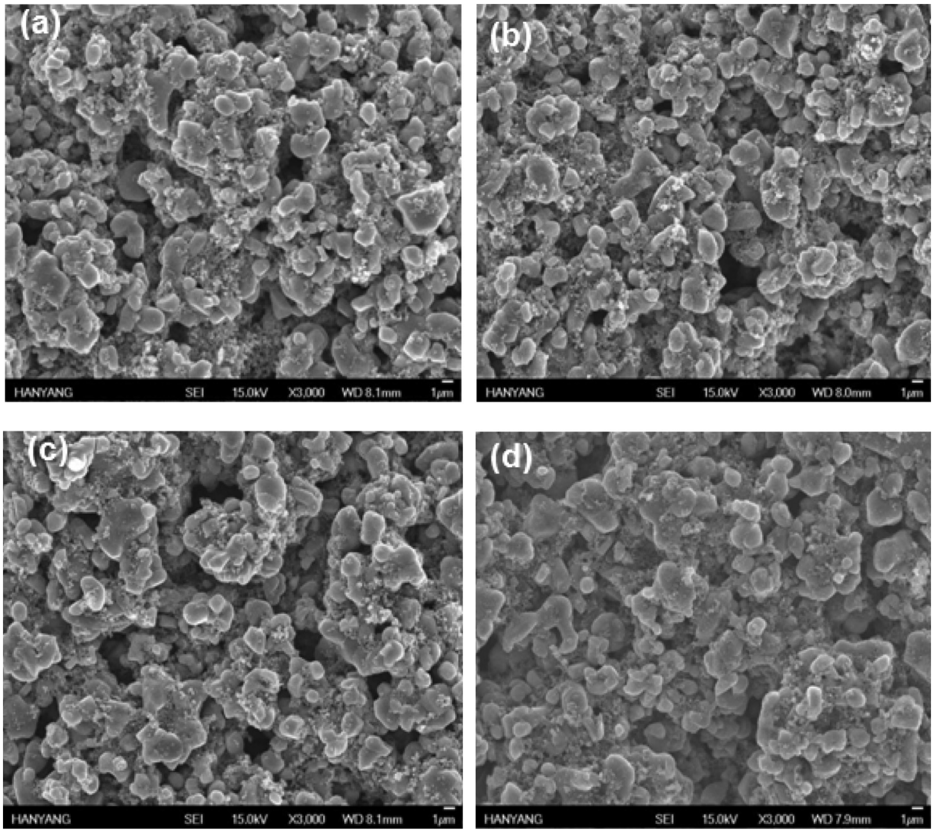

Fig. 6. SEM images of the surface of the $LiCoO_2$ cathodes after 100 cycles in different electrolytes: (a) base electrolyte and electrolyte solutions containing (b) BMP–TFSI, (c) BMP–PF_6, and (d) BMP–BF_4.

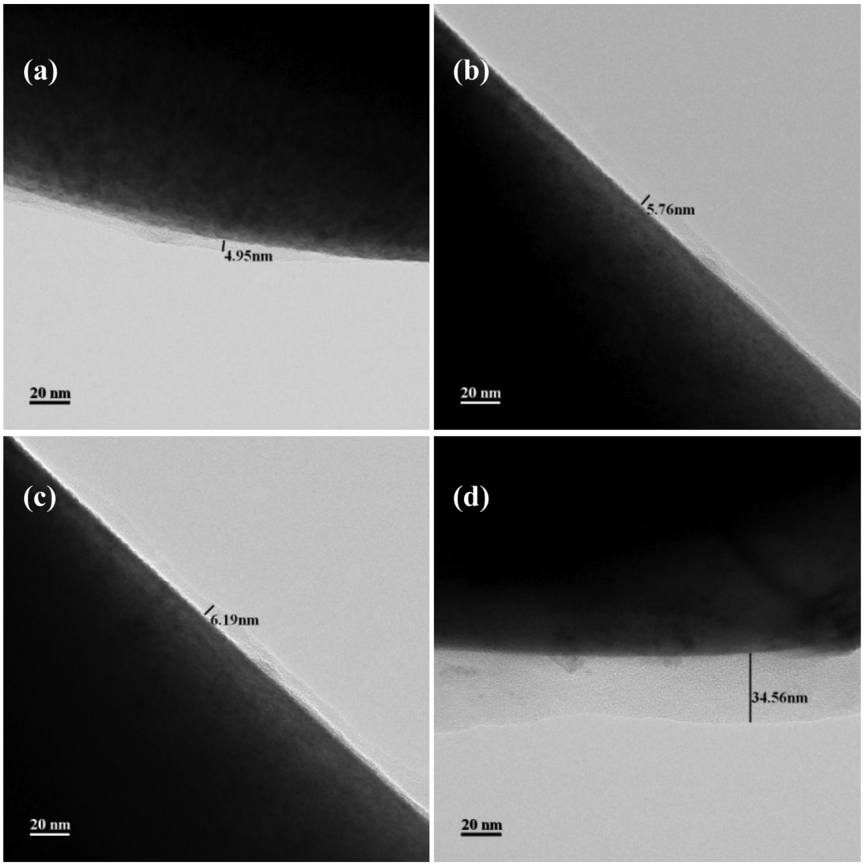

Fig. 7. TEM images of $LiCoO_2$ cathode active materials after 100 cycles in different electrolytes: (a) base electrolyte and electrolyte solutions containing (b) BMP–TFSI, (c) BMP–PF_6, and (d) BMP–BF_4.

The thermal stability of delithiated $Li_{1-x}CoO_2$ materials in the presence of the different electrolyte solutions was investigated. Fig. 8 compares the DSC profiles obtained after 100 cycles of the charged cathode materials in the electrolyte solutions containing the different ionic liquids. The DSC thermograms exhibit superimposed exothermic peaks, which reflect that the $Li_{1-x}CoO_2$ materials react with the electrolyte solution in multi-step processes, as reported earlier [16,28–30]. It is well known that the oxygen released from thermal decomposition of $Li_{1-x}CoO_2$ reacts vigorously with the organic solvents at high temperatures leading to highly exothermic reactions. It is clear that the thermal reactivity of $Li_{1-x}CoO_2$ and the electrolyte solution is affected by the presence of the ionic liquid. The overall exothermic heat generated by the thermal reaction of the charged cathode in the electrolyte solution containing ionic liquid is 248.0, 202.3 and 109.2 J g^{-1} for BMP–TFSI, BMP–PF_6 and BMP–BF_4, respectively, which are much lower than that measured in the base liquid electrolyte (437.7 J g^{-1}). Moreover, the onset temperature of the exothermic reactions shifted to higher temperatures with the addition of a small amount of ionic liquid. For example, the exothermic peaks in the electrolyte solution containing BMP–PF_6 shifted to higher temperatures about 14.3 and 34.2 °C, as compared to those of base electrolyte. These results suggest that the delithiated $Li_{1-x}CoO_2$ material is less reactive toward the electrolyte solution containing an ionic liquid, leading to an improved thermal stability. The thermal stability of the $Li_{1-x}CoO_2$ material was considerably improved in the electrolyte solution containing BMP–BF_4, although the cycling performance is the most inferior. This result reflects that the thick surface layer formed on the cathode materials (Fig. 7(d)) rendered the cathode materials less reactive toward the electrolyte solution.

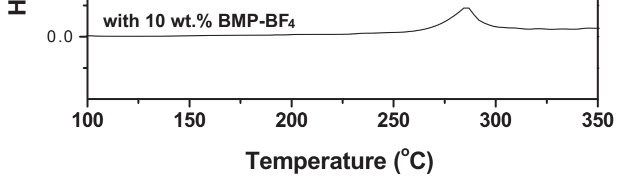

Fig. 8. DSC profiles of the $Li_{1-x}CoO_2$ cathode materials charged to 4.2 V after 100 cycles in the cells assembled with the electrolyte solutions containing different ionic liquids.

4. Conclusions

Electrolyte solutions containing different ionic liquids (BMP–TFSI, BMP–PF_6, BMP–BF_4) were prepared and their electrochemical characteristics were investigated. The addition of ionic liquid to the base electrolyte was effective in reducing the flammability of the electrolyte solution. The electrolyte solutions containing BMP–TFSI or BMP–PF_6 showed the electrochemical stabilities suitable for the operation of lithium-ion cells. The cycling tests and DSC results revealed that the addition of BMP–PF_6 to the base electrolyte could improve the safety without degrading the cycling performance of the cell. These results demonstrate that BMP–PF_6 is the most desirable ionic liquid as a flame-retarding additive for lithium-ion cells with good cycling performance and enhanced thermal stability.

Acknowledgments

This work was supported by the IT R&D program of MKE/KEIT (KI002176-2010-02) and by a grant from the National Research Foundation of Korea funded by the MEST of the Korean Government (NRF-2009-C1AAA001-0093307).

References

[1] J. Yamaki, I. Yamazaki, M. Egashira, S. Okada, J. Power Sources 102 (2001) 288.
[2] K. Xu, C.A. Angell, J. Electrochem. Soc. 149 (2002) A920.
[3] T.H. Nam, E.G. Shim, J.G. Kim, H.S. Kim, S.I. Moon, J. Electrochem. Soc. 154 (2007) A957.
[4] D. Zhou, W. Li, C. Tan, X. Zuo, Y. Huang, J. Power Sources 184 (2008) 589.
[5] A. Guerfi, S. Duchesne, Y. Kobayashi, A. Vijh, K. Zaghib, J. Power Sources 175 (2008) 866.
[6] T. Tsujikawa, K. Yabuta, T. Matsushita, T. Matsushima, K. Hayashi, M. Arakawa, J. Power Sources 189 (2009) 429.
[7] Y. Shigematsu, M. Ue, J. Yamaki, J. Electrochem. Soc. 156 (2009) A176.
[8] J.Y. Mun, Y.S. Jung, T. Yim, H.Y. Lee, H.J. Kim, Y.G. Kim, S.M. Oh, J. Power Sources 194 (2009) 1068.
[9] S.Y. Chen, Z.X. Wang, H.L. Zhao, H.W. Qiao, H.L. Luan, L.Q. Chen, J. Power Sources 187 (2009) 229.
[10] J.A. Choi, Y.K. Sun, E.G. Shim, B. Scrosati, D.W. Kim, Electrochim. Acta 56 (2011) 10179.
[11] M. Galinski, A. Lewandowski, I. Stepniak, Electrochim. Acta 51 (2006) 5567.
[12] A. Lewandowski, A. Swiderska-Mocek, J. Power Sources 194 (2009) 601.
[13] M. Armand, F. Endres, D.R. MacFarlane, H. Ohno, B. Scrosati, Nat. Mater. 9 (2009) 621.
[14] J.H. Shin, E.J. Cairns, J. Power Sources 177 (2008) 537.
[15] P. Reale, A. Fernicola, B. Scrosati, J. Power Sources 194 (2009) 182.
[16] L. Larush, V. Borgel, E. Markevich, O. Haik, E. Zinigrad, D. Aurbach, J. Power Sources 189 (2009) 217.
[17] J. Hassoun, A. Fernicola, M.A. Navarra, S. Panero, B. Scrosati, J. Power Sources 195 (2010) 574.
[18] Y.S. Yun, J.H. Kim, S.Y. Lee, E.G. Shim, D.W. Kim, J. Power Sources 196 (2011) 6750.
[19] S.M. Eo, E. Cha, D.W. Kim, J. Power Sources 189 (2009) 766.
[20] K. Xu, M.S. Ding, S. Zhang, J.L. Allen, T.R. Jow, J. Electrochem. Soc. 149 (2002) A622.
[21] H.F. Xiang, H.Y. Xu, Z.Z. Wang, C.H. Chen, J. Power Sources 173 (2007) 562.
[22] S. Chen, Z. Wang, H. Zhao, H. Qiao, H. Luan, L. Chen, J. Power Sources 187 (2009) 229.
[23] S.R. Sivakkumar, D.R. MacFarlane, M. Forsyth, D.W. Kim, J. Electrochem. Soc. 154 (2007) A834.
[24] R. Mogi, M. Inaba, S.K. Jeong, Y. Iriyama, T. Abe, Z. Ogumi, J. Electrochem. Soc. 149 (2002) A1578.
[25] T. Sato, T. Maruo, S. Marukane, K. Takagi, J. Power Sources 138 (2004) 253.
[26] M. Holzapfel, C. Jost, A. Prodi-Schwab, F. Krumeich, A. Wursig, H. Buqa, P. Novak, Carbon 43 (2005) 1488.
[27] I.A. Profatilova, N.S. Choi, S.W. Roh, S.S. Kim, J. Power Sources 192 (2009) 636.
[28] Y. Baba, S. Okada, J. Yamaki, Solid State Ionics 148 (2002) 311.
[29] D.D. MacNeil, J.R. Dahn, J. Electrochem. Soc. 149 (2002) A912.
[30] J. Jiang, J.R. Dahn, Electrochim. Acta 49 (2004) 2661.